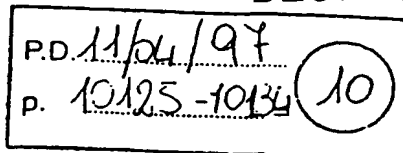


XP-002104482



THE JOURNAL OF BIOLOGICAL CHEMISTRY
© 1997 by The American Society for Biochemistry and Molecular Biology, Inc.

Vol. 272, No. 15, Issue of April 11, pp. 10125-10134, 1997
Printed in U.S.A.

The First Immunoglobulin-like Neural Cell Adhesion Molecule (NCAM) Domain Is Involved in Double-reciprocal Interaction with the Second Immunoglobulin-like NCAM Domain and in Heparin Binding*

(Received for publication, June 6, 1996, and in revised form, December 26, 1996.)

Vladislav V. Kiselyov†, Vladimir Berezin, Thomas E. Maar, Vladislav Soroka, Klaus Edvardsen, Arne Schousboe§, and Elisabeth Bock

From the Protein Laboratory, Panum Institute, University of Copenhagen, Blegdamsvej 3C, Building 6.2, DK-2200 Copenhagen, and the §Department of Biology, Royal Danish School of Pharmacy, Universitetsparken 2, DK-2100 Copenhagen, Denmark

To study the function of the first immunoglobulin (Ig)-like domain of the neural cell adhesion molecule (NCAM), it was produced as a recombinant fusion protein in a bacterial expression system and as a recombinant protein in a eukaryotic expression system of the yeast *Pichia pastoris*. For comparison, other NCAM domains were also produced as fusion proteins. By means of surface plasmon resonance analysis, it was shown that the first Ig-like NCAM domain binds the second Ig-like NCAM domain with a dissociation constant $5.5 \pm 1.6 \times 10^{-5}$ M. Furthermore, it was found that the first Ig-like domain binds heparin. It was also demonstrated that the second Ig-like NCAM domain binds heparin and that both domains bind collagen type I via heparin but not collagen type I directly.

The neural cell adhesion molecule (NCAM)¹ is a cell surface glycoprotein belonging to the immunoglobulin (Ig) superfamily (1, 2). It consists of five Ig-like domains and two fibronectin type III repeats (3, 4). The structure of the first Ig-like domain (IgI) belongs to the intermediate set of Ig-like domains (5). NCAM is expressed as three major isoforms: two transmembrane isoforms NCAM-A (180 kDa) and NCAM-B (140 kDa), and a glycosylphosphatidylinositol-anchored NCAM-C (120-kDa) isoform.

NCAM is known to mediate cell-cell interactions by a Ca^{2+} -independent homophilic binding mechanism (6–8). The mechanism of this binding is not clear. It has been reported that a sequence of 10 amino acids in the IgIII domain of chick NCAM is involved in the homophilic binding (9, 10). In another study, it was demonstrated that all five Ig-like domains of chick NCAM were involved in this binding (11). However, analysis of the structure of the IgI domain, determined by NMR spectroscopy, and the predicted structure of the IgII domain of mouse NCAM suggests that an acidic cluster of residues at the NH_2 -terminal of the IgI domain (aspartic acid 29, 32, 34, 58, 59, 84; glutamic acid 85) and a basic cluster of residues of the IgII

domain (lysine 135, 137, 185; arginine 139, 171) may be involved in a symmetrical double-reciprocal binding (5).

NCAM also mediates cell-substratum interactions. Different types of collagen have been shown to bind NCAM (12), but a collagen binding site in NCAM has not been identified. NCAM also binds heparin/heparan sulfate (13–15) and chondroitin sulfate proteoglycans (15, 16). The heparin binding domain was initially localized to a 25-kDa NH_2 -terminal fragment of NCAM (17) and, later, mapped to a 17-amino acid long region of the IgII domain (18).

The IgI domain of NCAM has been produced as a recombinant polypeptide in a bacterial expression system (19). When used as a substratum, this construct promoted adhesion of neuronal cell bodies, modified the migration pattern of cells from cerebellar microexplants, and increased metabolism of inositol phosphates and intracellular concentrations of Ca^{2+} and pH, thus indicating a functional importance of this domain (19).

The limited data concerning binding properties of the IgI NCAM domain have prompted us to investigate further the role of this domain in NCAM-mediated binding interactions. We therefore produced the IgI NCAM domain as a recombinant fusion protein in a bacterial expression system and as a recombinant protein in a eukaryotic expression system of the yeast *Pichia pastoris*. For comparison, other NCAM domains were also produced as fusion proteins. Both the IgI and IgII domains inhibited aggregation of cerebellar neurons, whereas other Ig-like domains of NCAM did not, indicating that the IgI and IgII domains were functionally active. Using surface plasmon resonance analysis, we show that the IgI domain binds the immobilized IgII domain and, *vice versa*, the IgII domain binds the immobilized IgI domain. We also show that IgI and IgII domains bind heparin and, via heparin, collagen type I but not collagen type I directly.

EXPERIMENTAL PROCEDURES

Production of Fusion Proteins of NCAM Fragments in a Bacterial Expression System

Construction of Fusion Proteins—Six fusion proteins were produced using mouse NCAM cDNA encoding the NCAM-C 120-kDa isoform (20, kindly provided by Dr. C. Goridis, Laboratoire de Genetique et Physiologie du Developpement, CNRS-Universite Aix-Marseille-II, Luminy) or the NCAM-B 140-kDa isoform (21, kindly provided by Dr. W. Wille, Institut für Genetik der Universität zu Köln). The fusion proteins consisted of an NCAM fragment fused between *Escherichia coli* maltose-binding protein (MBP) and an NH_2 -terminal fragment (65 amino acids) of *E. coli* β -galactosidase. The cDNA for the IgI domain was excised from NCAM-C cDNA with the *Pst*I and *Hinc*II restriction enzymes, and the cDNA fragments for NCAM domains IgII, IgIII, IgIV (including exon VASE), IgV, and the intracellular part of NCAM-B (Ex16,17,19) were synthesized by the polymerase chain reaction. The

This work was supported by the EU Program on *In Vitro* Developmental Toxicology Contract BIO2-CT-93-0471, the EU Program on Neuronal Development and Regeneration Contract BIO2-CT-93-0260, the Danish Medical Research Council, the Danish Biotechnology Program, the Danish Cancer Society, and the Lundbeck Foundation. The costs of publication of this article were defrayed in part by the payment of page charges. This article must therefore be hereby marked "advertisement" in accordance with 16 U.S.C. Section 1734 solely to indicate this fact.

* To whom correspondence should be addressed.

† The abbreviations used are: NCAM, neural cell adhesion molecule; Ig, immunoglobulin; MBP, maltose-binding protein; PSA, polysialic acid.

cDNA fragments were subcloned into a pMAL-c expression vector (New England Biolabs). The template for polymerase chain reaction amplification of the cDNA for Ex16,17,19 was the NCAM-B cDNA. For the other constructs the template was the NCAM-C cDNA. An XL1-Blue strain of *E. coli* (Stratagene) was used for the transformation with the recombinant and control pMAL-c plasmids. The recombinant clones were identified by small scale expression of the fusion proteins. Production of a fusion protein containing NCAM fibronectin type III domains I and II has been described previously (22). The fusion proteins were designated Ig_n-MBP (Ig-like domain number *n* produced in *E. coli* as a fusion protein with MBP as a fusion partner); Ex16,17,19-MBP (polypeptide encoded by NCAM exons 16, 17, and 19 produced in *E. coli* as a fusion protein with MBP as a fusion partner); and F31,II-MBP (fibronectin type III domains I and II produced in *E. coli* as a fusion protein with MBP as a fusion partner). For IgI-MBP, IgII-MBP, and IgIII-MBP, the recombinant pMAL-c plasmids were sequenced. IgII-MBP *E. coli* did not contain the β -galactosidase fragment because insertion of the IgII cDNA into the pMAL-c plasmid resulted in a shift of the reading frame terminating the β -galactosidase after seven amino acids.

Expression and Purification of the Fusion Proteins.—*E. coli* cells propagating the recombinant and control pMAL-c plasmids were grown in Terrific Broth (Sigma) containing 50 μ g/ml ampicillin at 37 °C. Cells were induced for 2 h with 1 mM isopropyl- β -D-thiogalactopyranoside and thereafter harvested by centrifugation and resuspended in 10 mM sodium phosphate, pH 7.4, 30 mM NaCl, 10 mM EDTA. Cells were subsequently frozen at -20 °C and thawed at room temperature. The sample was sonicated intermittently for 2 min on ice and centrifuged at 27,000 \times g for 30 min at 4 °C. The supernatant was saved for purification of the fusion protein.

An amylose resin column (New England Biolabs) was equilibrated with column buffer 1 (10 mM sodium phosphate, pH 7.4, 0.5 M NaCl, 2 mM EDTA). The supernatant was diluted to 2–3 mg/ml total protein with column buffer 1 and loaded onto the column. The column was first washed with column buffer 1 until A_{280} was less than 0.03 and then with 3 column volumes of column buffer 2 (10 mM sodium phosphate, pH 7.4, 100 mM NaCl). Finally, the fusion protein was eluted with column buffer 2 containing 10 mM maltose. The eluted protein was concentrated to 5–10 mg/ml and stored frozen at -20 °C. The yield was 30–100 mg of purified protein/liter of bacterial culture.

Production of the IgI NCAM Domain in the *P. pastoris* Yeast Expression System

Construction of the Recombinant Protein.—The IgI domain of NCAM was also produced as a recombinant protein (without MBP as a fusion partner) in *P. pastoris*. The cDNA fragment was synthesized by polymerase chain reaction. The amplified cDNA was subcloned into an *Xba*I/*Bam*HI site of the pHIL-S1 plasmid (Invitrogen Corporation, San Diego). An *E. coli* strain Top 10 F⁺ (Invitrogen) was used for transformation, and the recombinant clones were identified by restriction analysis of the plasmid DNA. The recombinant plasmid was linearized with *Nsi*I and used for transfection of a *P. pastoris* strain His 4 GS-115 (Invitrogen). Transfection and selection were performed according to a *Pichia* expression kit manual supplied by the manufacturer. The recombinant protein was designated as IgI *P. pastoris* (Ig-like domain I produced in *P. pastoris*). The authenticity of IgI *P. pastoris* was secured by amino acid sequencing and mass spectroscopy confirming the expected molecular mass of 11 kDa.

Expression and Purification of the Secreted Protein.—Cells were grown in 50 ml of medium A (13.4 g of yeast nitrogen base without amino acids (Difco, Detroit), 2 ml of 0.02% biotin, 20 g of glycerol, 40 mg of tryptophan, 50 mg of glutamic acid, 50 mg of methionine, 50 mg of lysine, 50 mg of leucine, 50 mg of isoleucine/liter of 100 mM potassium phosphate, pH 6.0) at 30 °C until saturation ($A_{600} \approx 5.0$). 10 ml of the saturated culture was transferred into 300 ml of medium A and incubated for 24 h at 30 °C. Cells were then centrifuged at 2,000 \times g for 10 min at 20 °C and resuspended in 50 ml of medium B (the same as medium A except that 20 g of 100% methanol was used instead of 20 g of glycerol). After incubation for 24 h at 30 °C, cells were pelleted by centrifugation at 3,000 \times g for 20 min at 20 °C, and the supernatant was filtered through a 0.22- μ m filter and concentrated to 2–3 mg of total protein/ml. The IgI *P. pastoris* was purified by gel filtration using a Sephadex G-50 column (Pharmacia Biotech Inc.) and stored frozen at -20 °C. The yield was 40–50 mg of purified protein/liter of cell culture.

Production of Antibodies

Polyclonal rabbit antibodies were raised against IgI-MBP. Rabbits were immunized as described (23).

Immunoblotting

Proteins, separated on 7.5% (w/v) polyacrylamide gels (24), were electroblotted onto a polyvinylidene difluoride membrane (Millipore, Bedford, MA). Nonspecific binding was blocked by incubation with 2% Tween 20 in washing buffer (50 mM Tris-HCl, pH 10.2, 450 mM NaCl, 0.2 mM phenylmethylsulfonyl fluoride). After washing, the membrane was incubated overnight on a shaking platform with either a rabbit antiserum against IgI-MBP diluted 1:200 or with polyclonal rabbit antibodies against rat NCAM (25) diluted 1:2,000. Alkaline phosphatase-conjugated swine anti-rabbit IgG (Dakopatts, Denmark) were used as secondary antibodies in a dilution of 1:2,000. After washing, the membrane was incubated in a staining buffer consisting of 0.1 M ethanolamine HCl, pH 9.6, 0.1 mM nitroblue tetrazolium, 0.15 mM 5-bromo-4-chloro-3-indolyl phosphate, 2 mM MgCl₂, 1% methanol, 0.5% acetone.

Assay for Aggregation of Cerebellar Neurons

Mixed primary microwell cultures of dissociated mouse cerebellum were prepared as described previously (26). Briefly, a suspension of dissociated cells from cerebella of 6-day-old mice was plated onto an uncoated 60-well microtiter plate (Nunc, Denmark) at a density of 45,000 cells/well in a volume of 10 μ l. Cells were grown for 24 h in a culture medium consisting of Dulbecco's modified Eagle's medium supplemented with 19 mM KCl, 25 mM glucose, 0.2 mM glutamine, 0.1 international unit/liter insulin, 0.15 mM *p*-aminobenzoate, 100 international units/ml penicillin, and 10% (v/v) fetal calf serum. Various protein constructs were added to the culture medium before plating at the indicated concentrations. The number of aggregates, defined as clusters of more than 50 cells, was determined after 24 h of incubation.

Surface Plasmon Resonance Analysis

Real time biomolecular interaction analysis was performed using a BIAcore instrument (Pharmacia Biosensor AB, Sweden). All of the experiments were performed at 25 °C using Hepes-buffered saline (10 mM Hepes, pH 7.4, 150 mM NaCl, 3.4 mM EDTA, 0.005% v/v Surfactant P20 (Pharmacia Biosensor)) as a running buffer. The flow rate was, unless otherwise specified, 5 μ l/min.

Immobilization of Collagen Type I.—Collagen type I, purified from rat tails (27), was immobilized on a sensor chip CM5 (Pharmacia Biosensor) using the following procedure. The chip was activated by 10 μ l of 0.05 M *N*-hydroxysuccinimide, 0.2 M *N*-ethyl-*N'*-dimethylaminopropyl carbodiimide. Collagen type I was immobilized using 15 μ l of 40 μ g/ml collagen type I in 10 mM sodium acetate buffer, pH 5.5. Finally the chip was blocked by 15 μ l of 1 M ethanolamine HCl, pH 8.5.

Binding of Fusion Proteins of NCAM Fragments to Collagen-Heparin Complex.—Heparin was bound to collagen type I immobilized on a CM5 sensor chip using 50 μ l of 10 mg/ml heparin from porcine intestinal mucosa (Sigma) dissolved in MilliQ water. Subsequently, 65 μ l of a fusion protein at 100 μ g/ml concentration was applied. In a competition experiment, IgI-MBP or IgII-MBP at 100 μ g/ml concentration was preincubated with 100 μ g/ml heparin for 15 min. The chip was regenerated by four 5- μ l pulses of 50 mM NaOH.

Binding of IgI *P. pastoris* and Fusion Proteins of NCAM Fragments to Heparin.—Heparin was biotinylated by mixing 1 mg of heparin/ml with 0.75 mM biotinamidocaproate *N*-hydroxysuccinimide ester (Sigma), 0.1 M sodium borate buffer, pH 8.8, for 1 h at room temperature. Biotinylated heparin was separated from the free biotinylation reagent by gel filtration using a Sephadex G-25 M column (Pharmacia). Heparin was immobilized injecting 25 μ l of 10 μ g/ml biotinylated heparin into an SA5 sensor chip (Pharmacia Biosensor) with preimmobilized streptavidin. Subsequently, 60 μ l of IgI *P. pastoris* at a flow rate of 30 μ l/min or 70 μ l of a fusion protein at a flow rate of 5 μ l/min was applied using the indicated concentrations. In a competition experiment, IgI-MBP or IgII-MBP at a 100 μ g/ml concentration was preincubated with either 500 μ g/ml heparin or polysialic acid (PSA) (Sigma) for 15 min, and IgI *P. pastoris* at a concentration of 100 μ g/ml was preincubated with 200 μ g/ml heparin for 5 min. Finally the chip was regenerated by three 5- μ l pulses of 50 mM NaOH.

Binding of Various Fusion Proteins of NCAM Domains to IgI-MBP or IgII-MBP.—IgI-MBP and IgII-MBP were biotinylated by mixing 1 mg of fusion protein/ml with 0.05 mM biotinamidocaproate *N*-hydroxysuccinimide ester in Hepes-buffered saline for 1 h at 4 °C. The biotinylated fusion protein was separated from the free biotinylation reagent by gel filtration using a Sephadex G-25 M column. The biotinylated IgI-MBP or IgII-MBP was immobilized injecting 100 μ l of 10 μ g/ml biotinylated fusion protein into an SA5 sensor chip at a flow rate of 2 μ l/min. Subsequently, different fusion proteins of NCAM fragments in Hepes-buffered saline containing 2.2 mM maltose were injected into a sensor

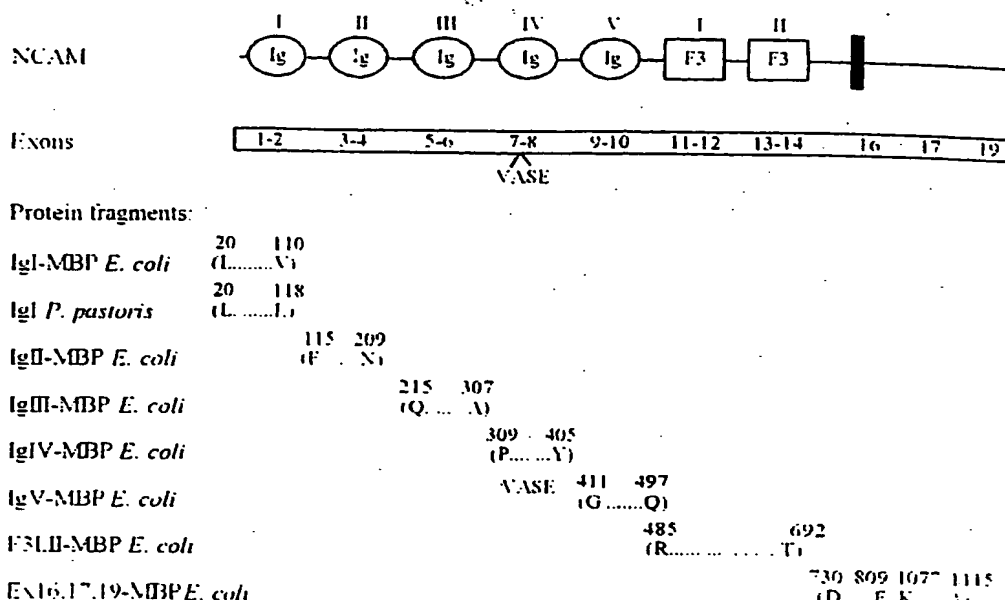


FIG. 1. Schematic structure of mouse NCAM domains and exons and derivation of the corresponding recombinant NCAM constructs. IgI *P. pastoris*, residues 20-118; IgII-MBP, residues 115-209; IgIII-MBP, residues 215-307; IgIV-MBP, residues 309-405 (including exon VASE (ASWTRPEKQE) between residues 354 and 355); IgV-MBP, residues 411-497; F3.II-MBP, residues 485-692; Ex16,17,19-MBP, residues 730-809, 1077-1115. The numbering of amino acid residues is according to GenBank/EMBL under Accession No. A44290. Number 1 refers to the first amino acid of the secretion signal.

chip with either immobilized IgI-MBP (70 μ l injection) or IgII-MBP (50 μ l injection) at the indicated concentrations. Finally, the chip was regenerated by three 5- μ l pulses of 5 mM NaOH.

Data were analyzed by nonlinear curve fitting using the BIAevaluation Software Set (Pharmacia Biosensor). The dissociation rate constant (k_d) was calculated by fitting dissociation data to Equation 1, using k_a as a floating parameter

$$R(t) = R_{\infty} e^{-k_d(t-t_0)} \quad (\text{Eq. 1})$$

where R is response, t is time, R_{∞} is the response at the start of dissociation, and t_0 is the start time for the dissociation. The association rate constant (k_a) was calculated by fitting data to Equation 2, using k_d and R_{∞} (steady-state response level) as floating parameters

$$R(t) = R_{\infty} (1 - e^{-k_a C(t-t_0)}) \quad (\text{Eq. 2})$$

where C is concentration of the binding protein and t_0 is the start time for the association. The initial binding rate (r_0) was calculated by fitting data to Equation 3, using k_d and k_a as floating parameters

$$R(t) = \frac{r_0}{k_d} (1 - e^{-k_d t}) \quad (\text{Eq. 3})$$

where $k_d = k_{-1} C - k_{+1}$.

Estimation of the solution affinity of IgII-MBP to IgI *P. pastoris* was performed as described [35]. Briefly, the initial binding rate (r_0) of soluble IgII-MBP to immobilized IgI-MBP was determined at 1.79, 3.57, 5.36, 7.14, and 8.93 μ M concentrations of IgII-MBP. r_0 was plotted versus the concentration of IgII-MBP, fitted to a straight line, and the intercept (I) and slope (k) were estimated. Next, IgII-MBP at a 8.93 μ M concentration was mixed with IgI *P. pastoris* at 300, 150, 75, 37.5, 18.8, 9.4, and 4.7 μ M concentrations and incubated for 4 h at room temperature to reach equilibrium. r_{∞} of the binding of unbound IgII-MBP to immobilized IgI-MBP was determined for each concentration of IgI *P. pastoris*. r_{∞} was plotted versus total concentration (C) of IgI *P. pastoris*, and the data were fitted to Equation 4, using K_D (dissociation constant in solution) and r_{∞} (initial binding rate of IgII-MBP in the absence of IgI *P. pastoris*) as floating parameters.

$$r_{\infty}(C) = r_{\infty} - \frac{k}{2} \left(C - \frac{r_{\infty} - I}{k} - K_D \right)^2 - C \left(\frac{r_{\infty} - I}{k} \right) \quad (\text{Eq. 4})$$

RESULTS

To study the function of the IgI NCAM domain, it was synthesized in a bacterial expression system of *E. coli* as a recombinant fusion protein (IgI-MBP) and as a recombinant domain in a eukaryotic expression system of the yeast *P. pastoris* (IgI

P. pastoris). The fusion protein consisted of the IgI domain fused between *E. coli* MBP and an NH₂-terminal fragment (65 amino acids) of *E. coli* β -galactosidase. This expression system was chosen because it allows production of a large amount of soluble recombinant protein that can be purified by affinity chromatography using the natural affinity of MBP for maltose. The *P. pastoris* expression system was selected because *P. pastoris* is capable of protein folding and processing similar to higher eukaryotes [28], and the protein secreted into the medium can be purified easily. For comparison, we also produced other NCAM domains as fusion proteins: IgII-MBP, IgIII-MBP, IgIV-MBP, IgV-MBP, F3.II-MBP, and Ex16,17,19-MBP. The sequences of the various recombinant NCAM constructs are given in Fig. 1.

The recombinant NCAM constructs were purified and analyzed by SDS-polyacrylamide gel electrophoresis under reducing conditions as shown in Fig. 2, a and b. The purified proteins appeared to be more than 95% pure. The expected molecular masses for the constructed proteins were: MBP, ~52 kDa; IgII-MBP, ~56 kDa; IgI-MBP, IgIII-MBP, IgIV-MBP, and IgV-MBP, ~61-63 kDa; Ex16,17,19-MBP, ~64 kDa, and IgI *P. pastoris*, ~11 kDa. Only very small differences were observed between the calculated and the actual molecular masses probably because of aberrant electrophoretic migration. Characterization of F3.II-MBP has been described previously [22].

Polyclonal rabbit antibodies were raised against IgI-MBP. The antibodies of the first bleeding recognized NCAM from rat brain under nonreducing conditions but not NCAM treated with β -mercaptoethanol (Fig. 2c). The antibodies of the following bleedings recognized both nonreduced and reduced NCAM. This means that the antibodies of the first bleeding reacted with epitopes sensitive to reduction of the disulfide bond, indicating that they probably are conformational epitopes and that IgI-MBP employed for immunization was folded correctly.

Since NCAM mediates cell-cell interactions by a Ca²⁺-independent homophilic binding mechanism [6-8] and also cell-substratum interactions [12, 14, 16], we investigated a possible role of the IgI NCAM domain in these binding interactions.

The IgI and IgII NCAM Domains Inhibit Aggregation of Mouse Cerebellar Neurons—To test whether IgI-MBP and IgI *P. pastoris* were functionally active, the effects of the various NCAM domains on neuronal cell aggregation were tested. Since immobilized IgI and IgII domains have been demon-

strated to be most efficient (compared with other Ig-like NCAM domains) for adhesion of neuronal cell bodies (19), soluble IgI-MBP or IgI *P. pastoris* and IgII-MBP were expected to interfere with neuronal aggregation. Dissociated cells from cerebella of 6-day-old mice were plated on a microtiter plate and grown in the presence of various protein constructs; the number of cell aggregates was measured after 24 h of incubation. In the absence of any addition to the culture medium, cells initially spread evenly over the surface of the well, but after 24 h, large aggregates were formed. From Fig. 3a it appears that addition of IgI-MBP, IgII-MBP, and IgI *P. pastoris* inhibited the formation of aggregates and therefore led to a decrease in the size of aggregates and, as a result, to an increase in the number of smaller aggregates. IgIII-MBP and IgV-MBP did not have any effect when compared with MBP or phosphate-buffered saline, and IgIV-MBP had only a slight effect. To test whether MBP affects biological activity of the IgI domain in the IgI-MBP construct, a dose response of MBP, IgI-MBP, and IgI *P. pastoris* was studied. As appears from Fig. 3b, IgI-MBP and IgI *P. pastoris* had essentially the same dose-response curves, MBP alone had no effect at any of the tested doses, indicating that MBP does not affect biological activity of the IgI domain in the IgI-MBP construct. Thus, IgI-MBP, IgI *P. pastoris*, and

IgII-MBP NCAM domains inhibited aggregation of mouse cerebellar neurons, indicating that these protein constructs were functionally active and therefore suited for the subsequent binding assays.

The IgI Domain of NCAM Binds to Heparin—To test the possibility that the IgI NCAM domain is involved in NCAM-mediated heterophilic interactions, we used surface plasmon resonance analysis for studying the possible binding of this domain to some putative NCAM ligands. No binding was found to laminin, collagen type I, and fibronectin (not shown), whereas an affinity was found for heparin (Fig. 4a). To estimate the dissociation and association rate constants, we used the highest practically reasonable flow rate of 30 $\mu\text{L}/\text{min}$ to overcome possible mass transport limitation. The apparent constant of dissociation for IgI *P. pastoris* and the apparent association and dissociation rate constants, in the context of the model used (see "Experimental Procedures"), were $9.0 \pm 2.0 \times 10^{-7} \text{ M}$, $1.1 \pm 0.3 \times 10^4 \text{ M}^{-1} \text{ s}^{-1}$, and $8.4 \pm 0.4 \times 10^{-3} \text{ s}^{-1}$, respectively. The goodness of fit between the fitted curves and the experimental data was assessed by means of the χ^2 value defined as

$$\chi^2 = \frac{\sum_{i=1}^n (R_i^f - R_i^e)^2}{n - p} \quad (\text{Eq. 5})$$

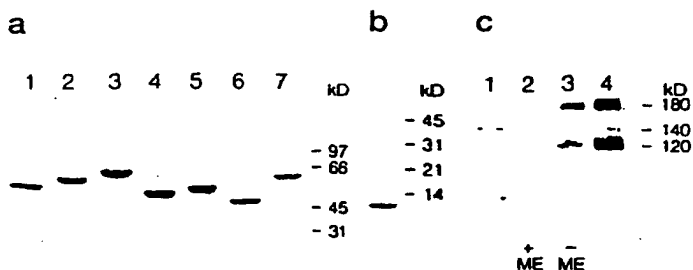


FIG. 2. Electrophoretic analysis of the purified NCAM constructs and immunoblotting analysis of the antibodies raised against the IgI-MBP. **Panel a.** 7.5% SDS-polyacrylamide gel electrophoresis of fusion proteins. Lane 1, IgV-MBP; lane 2, IgIV-MBP; lane 3, IgIII-MBP; lane 4, IgII-MBP; lane 5, IgI-MBP; lane 6, MBP; lane 7, Ex16,17,19-MBP. After electrophoresis the gel was stained with Coomassie Blue. **Panel b.** 20% SDS-polyacrylamide gel electrophoresis of IgI *P. pastoris*; the gel was stained with Coomassie Blue. **Panel c.** Immunoblotting of rat brain NCAM using the following antibodies: lane 1, rabbit antibodies against IgI-MBP from the tenth bleeding, the electrophoresis was conducted under reducing conditions; lane 2, antibodies from the same rabbit as in lane 1 but from the first bleeding, using reducing conditions; lane 3, the same antibodies as in lane 2, but under nonreducing conditions; lane 4, rabbit polyclonal antibodies against rat NCAM, using nonreducing conditions. ME stands for β -mercaptoethanol.

where R_i^f and R_i^e are the fitted and the experimental values, respectively; n and p are the number of data points and degrees of freedom, respectively. The χ^2 value was typically less than 1, indicating that the experimental data were described adequately by the equations of pseudo-first order kinetics (see "Experimental Procedures"). In a competition experiment, IgI *P. pastoris* was preincubated with soluble heparin for 5 min. This completely inhibited subsequent binding of IgI *P. pastoris* to immobilized heparin (Fig. 4a).

To compare the heparin binding of the IgI domain to the well documented heparin binding of the IgII domain (18), we used IgI-MBP and IgII-MBP and five control proteins: MBP alone, Ex16,17,19-MBP, IgIII-MBP, IgIV-MBP, and IgV-MBP. The IgII-MBP exhibited a stronger binding to heparin than IgI-MBP; but the control proteins, MBP and Ex16,17,19-MBP, both exhibited a very low, probably unspecific, binding (Fig. 4b). The binding of IgIII-MBP, IgIV-MBP, and IgV-MBP was at the same level as that of MBP and Ex16,17,19-MBP (not shown). In a competition experiment, IgI-MBP and IgII-MBP were preincubated with either soluble heparin or a control negatively charged carbohydrate, PSA, for 15 min. Heparin completely inhibited subsequent binding of the fusion proteins to immobi-

FIG. 3. Effect of the Ig-like NCAM domains on mixed primary cell cultures of mouse cerebellar neurons. **Panel a.** IgI-MBP, IgI *P. pastoris*, IgII-MBP, IgIII-MBP, IgIV-MBP, IgV-MBP, and MBP were added to the culture medium before plating at a concentration of $0.2 \mu\text{M}$ ($10 \mu\text{g}/\text{ml}$) for fusion proteins and $2 \mu\text{g}/\text{ml}$ for IgI *P. pastoris*. **Panel b.** MBP, IgI-MBP, and IgI *P. pastoris* were added at 0.008, 0.04, 0.2, and $1 \mu\text{M}$ concentrations. The number of cell aggregates was measured after 24 h. Three independent experiments, each in 10 replicates, were performed. The data from different experiments were pooled. The results are shown as mean \pm S.E.

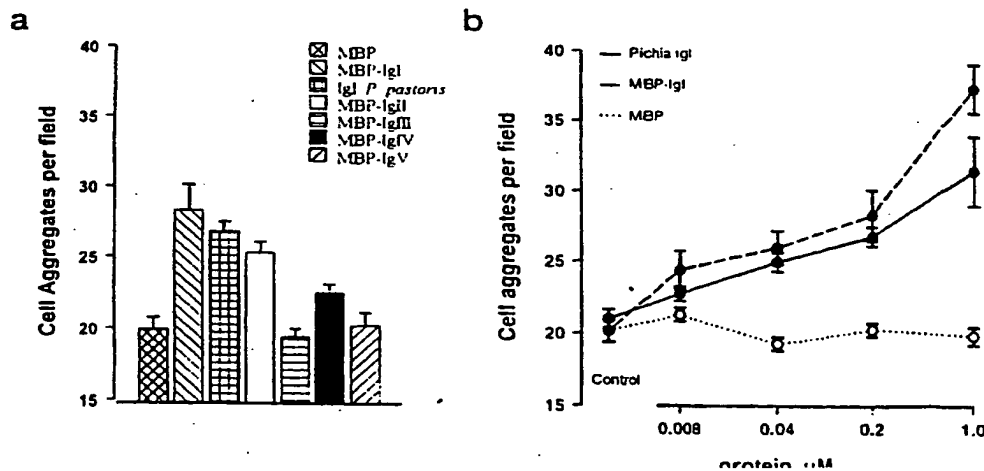
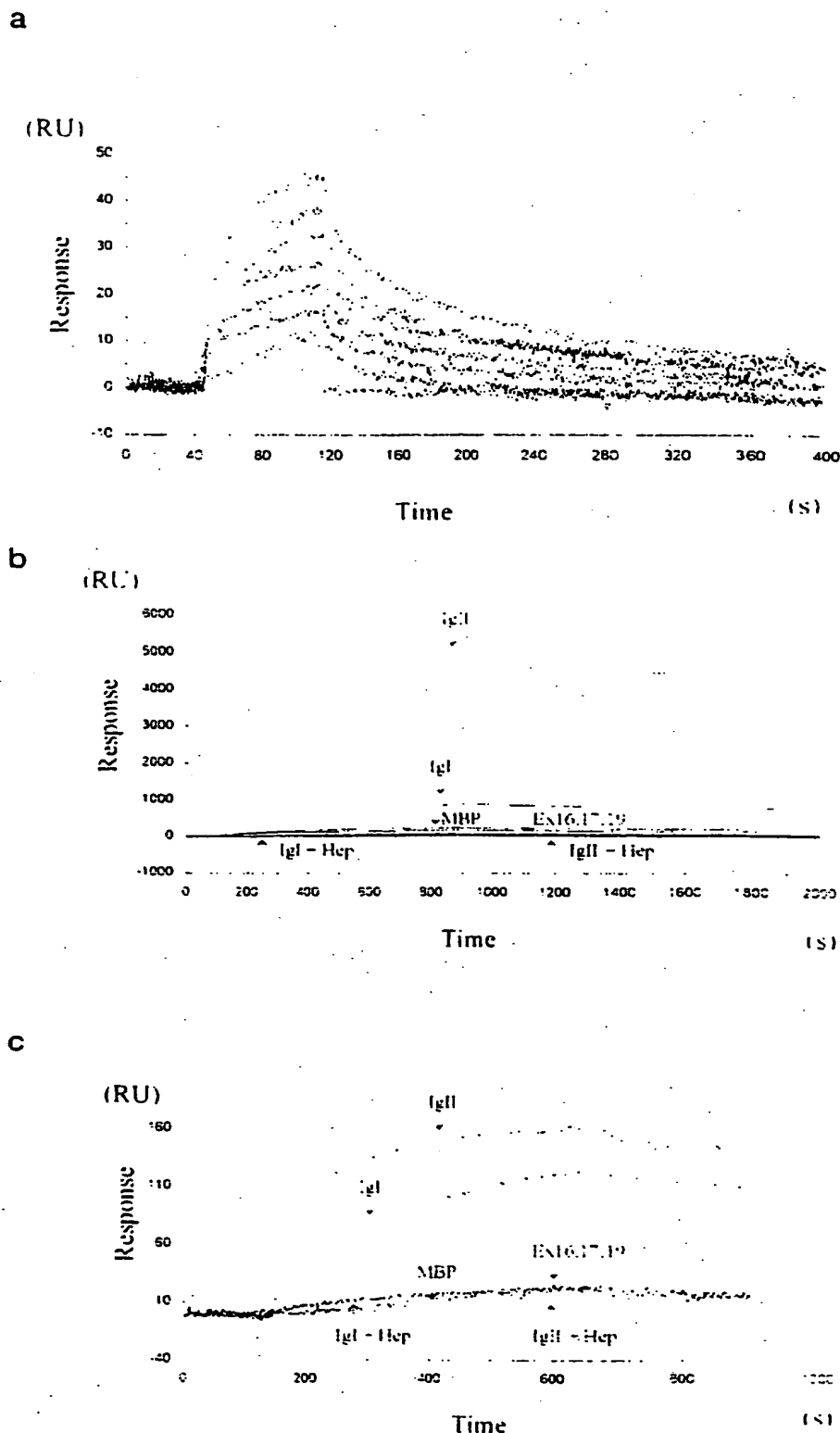


FIG. 4. Binding of Igl *P. pastoris*, IglI-MBP, and IglII-MBP to heparin or the collagen-heparin complex. Panel *a*, binding of Igl *P. pastoris* to immobilized heparin. The concentration of Igl *P. pastoris* (from top curve to bottom) was 10, 5, 3.5, 2, 1, and 0.5 μM , and 10 μM + 200 $\mu\text{g/ml}$ heparin. The Igl *P. pastoris* domain was tested for unspecific binding to a blank sensor chip and to a sensor chip with immobilized streptavidin at a concentration of 10 μM . No unspecific binding was detected. In a competition experiment, the Igl *P. pastoris* at a 10 μM concentration was preincubated with 200 $\mu\text{g/ml}$ heparin for 5 min. Two independent experiments were performed, and data from one of these experiments are presented. Panel *b*, binding of IglI-MBP and IglII-MBP to immobilized heparin. MBP and Ex16,17,19-MBP were used as controls. The concentration of each protein was 100 $\mu\text{g/ml}$. In a competition experiment, IglI-MBP or IglII-MBP at 100 $\mu\text{g/ml}$ was preincubated with 500 $\mu\text{g/ml}$ heparin for 15 min. The fusion proteins were tested for unspecific binding to a blank sensor chip and to a sensor chip with immobilized streptavidin. Only very low unspecific binding was detected. Three independent experiments were performed. The data from one representative experiment are shown. Panel *c*, binding of IglI-MBP and IglII-MBP to the collagen-heparin complex. MBP and Ex16,17,19-MBP were used as controls. The concentration of each protein was 100 $\mu\text{g/ml}$. In a competition experiment, IglI-MBP or IglII-MBP at 100 $\mu\text{g/ml}$ was preincubated with 100 $\mu\text{g/ml}$ heparin for 15 min. Three independent experiments were performed. The data from one representative experiment are shown.



lized heparin (Fig. 4b), whereas PSA had no effect (not shown). We were, however, unable to show binding of soluble heparin to either immobilized IglII-MBP or IglI-MBP. This may be because the surface of a CM5 sensor chip is negatively charged at pH 7.3. Since heparin molecules also are negatively charged, electrostatic repulsion between the surface of the sensor chip and heparin molecules may have precluded binding of heparin to IglI-MBP or IglII-MBP. It is also possible that the heparin binding

was not detected because of the low molecular mass of heparin since the observed signal in surface plasmon resonance analysis is proportional to the molecular mass of the soluble ligand, and/or the employed immobilization procedure may have inactivated the heparin binding sites of IglII-MBP and IglI-MBP.

We also tested whether IglI-MBP and IglII-MBP were able to bind a collagen-heparin complex. This was done by immobilizing collagen type I on the sensor chip and subsequently applying

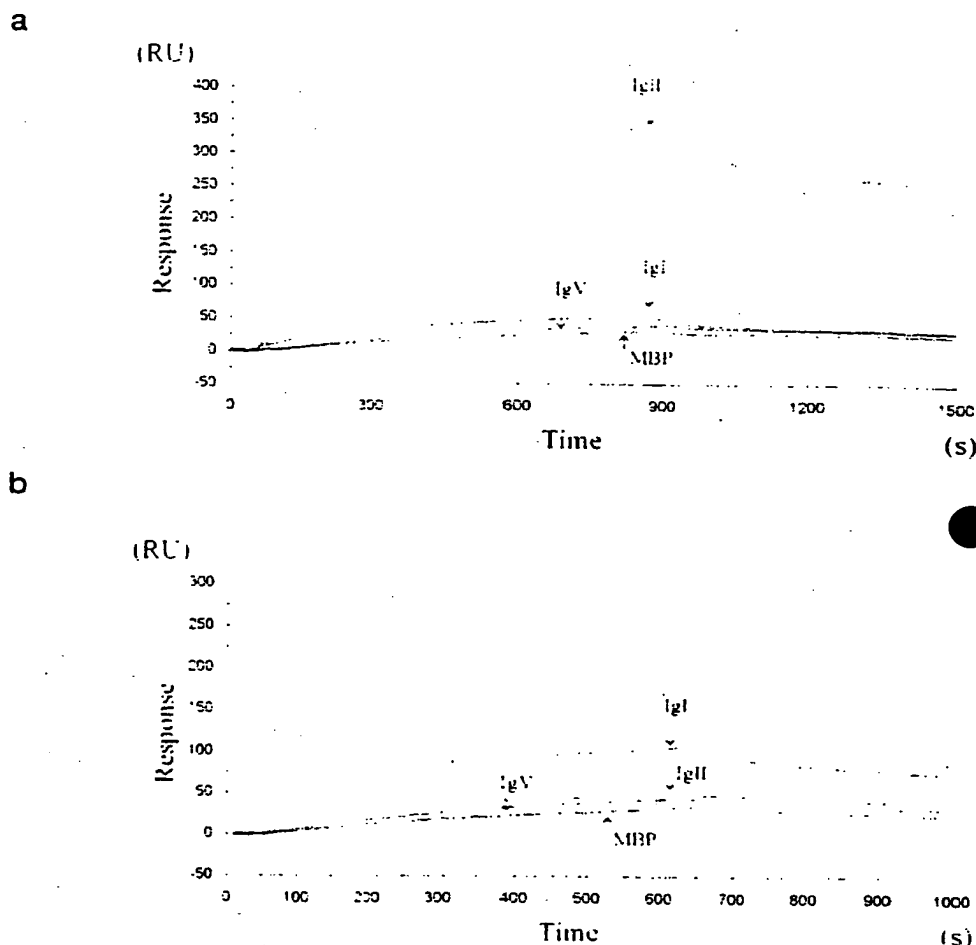


FIG. 5. Binding of fusion proteins of NCAM domains to immobilized IgI-MBP (panel a) and immobilized IgII-MBP (panel b). The concentration of the fusion proteins was 1 mg/ml (17 μ M). Three independent experiments were performed. The data from one representative experiments are shown.

ing heparin, which is a well known ligand of collagen (29). Although neither IgI-MBP nor IgII-MBP was able to bind to collagen type I directly, we found binding of IgI-MBP and IgII-MBP to the collagen-heparin complex (Fig. 4c). Interestingly, the maximal binding of IgII-MBP to heparin alone (Fig. 4b) was about ~5 times higher than the maximal binding of IgI-MBP, whereas the maximal binding of IgII-MBP to the collagen-heparin complex (Fig. 4c) was only 1.3 times higher than the maximal binding of IgI-MBP, indicating that IgI-MBP bound the collagen-heparin complex almost as well as IgII-MBP. This indicates that the IgI NCAM domain possibly also binds collagen type I although with a very low affinity.

In a competition experiment, IgI-MBP and IgII-MBP were preincubated with soluble heparin for 15 min. This completely inhibited subsequent binding of the fusion proteins to the collagen-heparin complex (Fig. 4c), indicating that it was heparin and not collagen type I that bound to IgI-MBP and IgII-MBP. The control proteins, MBP and Ex16.17.19-MBP, exhibited a very low, presumably unspecific binding to the sensor chip carrying the immobilized collagen-heparin complex (Fig. 4c); and the binding of IgIII-MBP, IgIV-MBP, IgV-MBP, and F3I.II-MBP was the same as that of the control proteins (not shown).

It was not possible to extract reliable kinetic data from the binding of IgI-MBP and IgII-MBP to either heparin alone or the collagen-heparin complex because of the interference of the MBP portion of IgI-MBP and IgII-MBP. MBP exhibited a low unspecific binding to heparin and the collagen-heparin complex compared with the binding of IgI-MBP and IgII-MBP (Fig. 4, b and c); however, the small amount of MBP that bound to heparin, did not dissociate. The dissociation of MBP and IgI-

MBP appeared to be identical (Fig. 4b), even though IgI *P. pastoris* dissociated from heparin very quickly with a dissociation rate constant of approximately 10^{-2} s^{-1} . We therefore believe that the dissociation rate of IgI-MBP was determined by the dissociation rate of the IgI domain and by the rate of very slow desorption of MBP. Therefore, it was not possible to calculate kinetic data reliably from the binding of fusion proteins containing MBP as a fusion partner. It should be mentioned that the maximal binding of IgI-MBP to heparin alone was approximately 900 resonance units, whereas the maximal binding of IgI-MBP to the collagen-heparin complex was only 120 resonance units. This was because in the former experiment, much more heparin was immobilized per area unit of the sensor chip than in the latter.

Thus, the IgI domain of NCAM bound heparin, although apparently with a lower affinity than the IgII NCAM domain. However, when heparin was bound to collagen type I, the IgI domain bound heparin almost as well as the IgII domain, indicating that the IgI domain possibly also recognized collagen type I although with a very low affinity.

The IgI NCAM Domain Is Directly Involved in NCAM-mediated Homophilic Binding—We finally tested the possibility that the IgI NCAM domain, may be involved in NCAM-mediated homophilic binding. IgI-MBP was immobilized on the sensor chip, and the binding of fusion proteins of various NCAM domains was tested at a concentration of 1 mg/ml. From Fig. 5a, it appears that IgII-MBP bound strongly to immobilized IgI-MBP, whereas IgI-MBP, IgV-MBP, and MBP exhibited low unspecific binding. The binding of IgIII-MBP, IgIV-MBP, and F3I.II-MBP was approximately the same as that of IgI-MBP.

FIG. 6. Estimation of the affinity of the IgI-IgII interaction. *Panel a.* binding of IgII-MBP at 35.7 μ M (2 mg/ml), 17.9, 8.9, 3.6, and 1.8 μ M concentrations to immobilized IgI-MBP. *Panel b.* binding of IgII-MBP at 8.9 μ M (0.5 mg/ml) concentration to immobilized IgI-MBP in the presence of IgI *P. pastoris* at 4.7, 9.4, 18.8, 37.5, 75, 150, and 300 μ M concentrations. IgII-MBP was preincubated with IgI *P. pastoris* for 4 h before measurement of the binding. Three independent experiments were performed. The data from one representative experiment are shown. *Panel c.* initial binding rate of IgII-MBP to immobilized IgI-MBP at various concentrations of IgII-MBP. *Panel d.* initial binding rate of IgII-MBP at 8.9 μ M (0.5 mg/ml) concentration to immobilized IgI-MBP in the presence of IgI *P. pastoris* at various concentrations. Three independent experiments were performed. The results are shown as mean \pm S.E. The data were fitted to the model (see "Experimental Procedures").

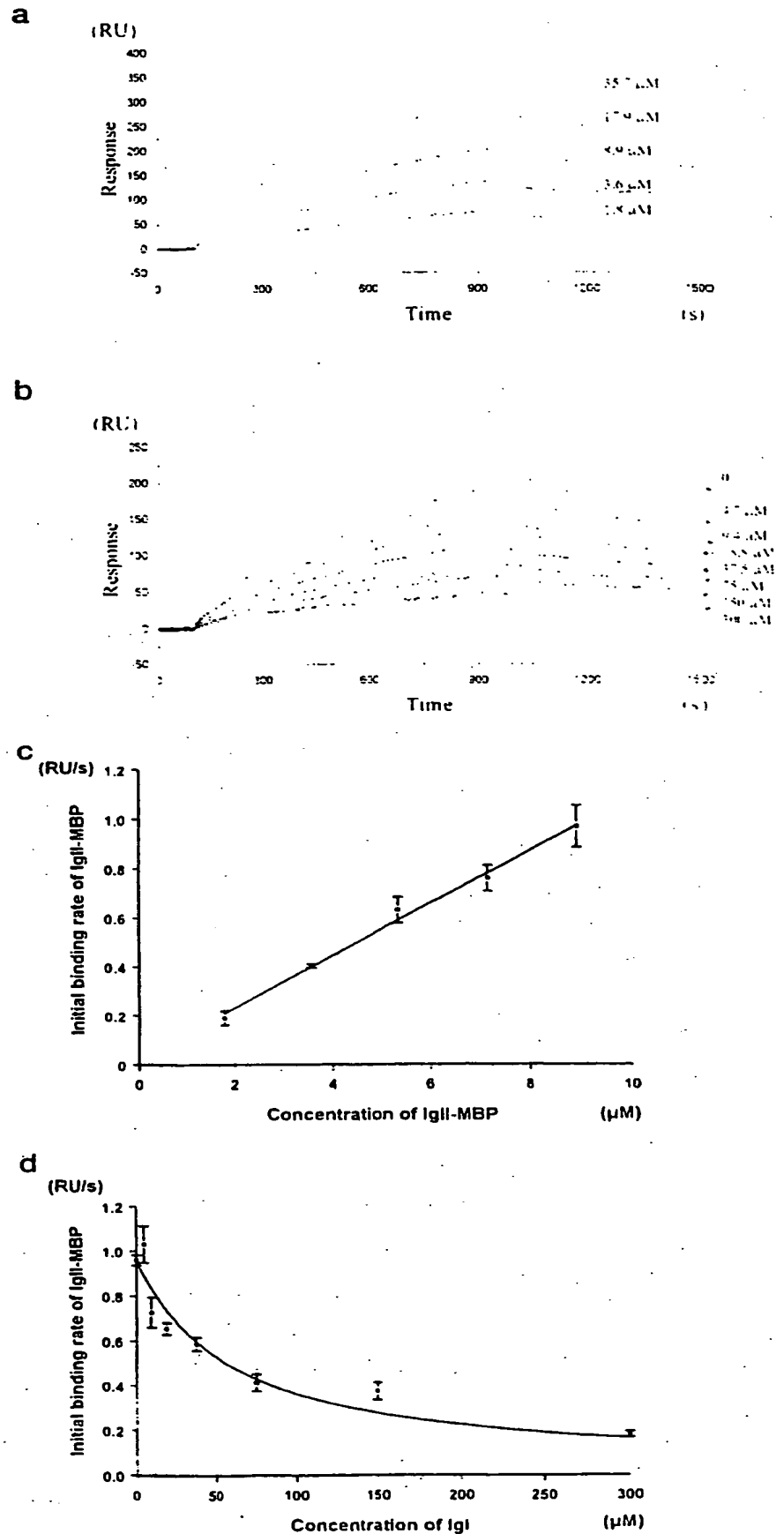
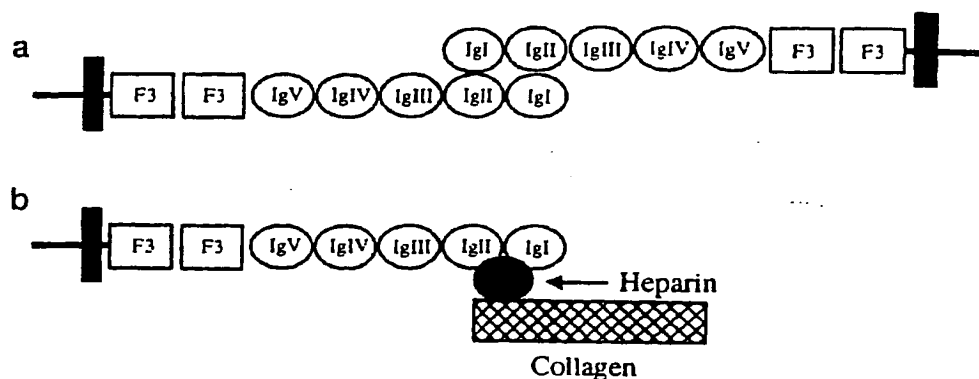


FIG. 7. Binding interactions of the IgI NCAM domain. Panel a, mechanism of NCAM-mediated homophilic binding: the IgI NCAM domain is involved in a symmetrical double-reciprocal interaction with the IgII NCAM domain. Panel b, mechanism of NCAM-collagen interaction: both the IgI and IgII NCAM domains bind to heparin and, via heparin, to collagen; thus, heparin forms a "bridge" between NCAM and collagen.



IgV-MBP, and MBP (not shown). Since soluble IgII-MBP binds to immobilized IgI-MBP, the reverse should also be expected, namely that soluble IgI-MBP binds to immobilized IgII-MBP. Therefore, we also immobilized IgII-MBP on the sensor chip and tested it for binding of various NCAM fusion proteins at a concentration of 1 mg/ml (Fig. 5b). IgI-MBP bound to immobilized IgII-MBP more strongly than IgII-MBP, IgV-MBP, and MBP, the maximal binding being at least two times higher than that of the other proteins. The binding of IgIII-MBP, IgIV-MBP, and F3I.II-MBP was approximately the same as that of the IgII-MBP, IgV-MBP, and MBP (not shown). It is easy to see that binding of soluble IgII-MBP to immobilized IgI-MBP was higher than binding of soluble IgI-MBP to immobilized IgII-MBP (Fig. 5, a and b). Since approximately the same amount of protein was immobilized in both cases, this difference in binding may be the result of partial inactivation of IgII-MBP and, possibly to a lesser extent, of IgI-MBP during immobilization. IgII-MBP might be more predisposed to partial inactivation during immobilization compared with IgI-MBP, because the fusion proteins were immobilized via amino groups of lysine residues, and the potential binding site of IgII-MBP is a cluster of basic amino acid residues consisting of lysine 135, 137, 185, and arginine 139 and 171 (5).

To determine the affinity of the IgI-IgII interaction, binding of soluble IgII-MBP to immobilized IgI-MBP was measured using various concentrations of IgII-MBP (Fig. 6a). The apparent dissociation constant and the apparent association and dissociation rate constants, in the context of the model used (see "Experimental Procedures"), were $1.3 \pm 0.3 \times 10^{-5}$ M, $1.4 \pm 0.3 \times 10^2$ M⁻¹ s⁻¹, and $1.2 \pm 0.1 \times 10^{-3}$ s⁻¹, respectively. The estimation of kinetic parameters from this experiment may not be reliable because of the interference of MBP. The rate of dissociation of IgII-MBP is determined by the rate of dissociation of the IgII domain and by the rate of unspecific desorption of MBP (see explanation above). This leads to underestimation of the dissociation rate constant (apparent slower dissociation) and, as a result, to overestimation of the affinity. Thus, the true value of the dissociation constant is higher than $1.3 \pm 0.3 \times 10^{-5}$ M.

To estimate the affinity of the IgI-IgII interaction more reliably, we therefore measured binding of IgII-MBP to IgI *P. pastoris* in solution, thus avoiding the problem of unspecific interaction of MBP with the sensor chip. IgII-MBP at an 8.93 μ M (0.5 mg/ml) concentration was mixed with various concentrations of IgI *P. pastoris*, incubated for 4 h at room temperature to reach equilibrium, and the binding of unbound IgII-MBP to immobilized IgI-MBP was measured at each concentration of IgI *P. pastoris* (Fig. 6b). To determine the concentration of unbound IgII-MBP in the mixture with IgI *P. pastoris*, a calibration of the initial binding rate of IgII-MBP to immobilized IgI-MBP versus the concentration of IgI-MBP

was performed (Fig. 6c). The initial binding rate of IgII-MBP to immobilized IgI-MBP in the mixture with IgI *P. pastoris* was calculated, plotted versus the concentration of IgI *P. pastoris*, and the data were fitted to the model (see "Experimental Procedures") (Fig. 6d), with the resulting dissociation constant of $5.5 \pm 1.6 \times 10^{-5}$ M. As expected, this value of dissociation constant was higher than $1.3 \pm 0.3 \times 10^{-5}$ M.

Since the IgIII domain of chick NCAM has been reported to bind to itself (9, 10), and the IgV, IgIV, IgII, and IgI domains of chick NCAM have been reported to bind to IgI, IgII, IgIV, and IgV, respectively (11), it was of interest to test whether the IgI, IgII, IgIII, IgIV, and IgV domains of mouse NCAM could bind to IgV, IgIV, IgIII, IgII, and IgI domains, respectively, under the chosen conditions. As shown above, soluble IgV-MBP and IgIV-MBP did not bind to immobilized IgI-MBP and IgII-MBP, respectively. When F3I.II-MBP, IgV-MBP, IgIV-MBP, and IgIII-MBP were immobilized, no specific binding of any domain was detected (not shown).

DISCUSSION

In this study we have investigated the role of the IgI NCAM domain in NCAM-mediated binding interactions. The functional activity of IgI-MBP and IgI *P. pastoris* was tested by studying the effects of the various NCAM domains on neuronal cell aggregation. IgI-MBP, IgI *P. pastoris*, and IgII-MBP inhibited aggregation of mouse cerebellar neurons, whereas other Ig-like domains of NCAM had very little, if any, effect, indicating that the IgI and IgII protein constructs were functionally active and therefore suited for the binding assays. The binding properties of the IgI NCAM domain were studied using surface plasmon resonance analysis, and it was demonstrated that IgI-MBP bound immobilized IgII-MBP, and vice versa, IgII-MBP bound immobilized IgI-MBP. It was also demonstrated that IgI *P. pastoris* inhibited binding of IgII-MBP to immobilized IgI-MBP. This indicates that the IgI and IgII domains are directly involved in homophilic interactions of NCAM. Our results are in agreement with Frei *et al.* (19), who showed that the IgI and IgII NCAM domains, synthesized in a bacterial expression system, when used as immobilized substratum, clearly promoted cell adhesion of NCAM-expressing cells, whereas other NCAM domains hardly had any adhesive effects. Our data are also in accordance with reports that a 25-kDa NH₂-terminal NCAM fragment containing the IgI and IgII NCAM domains is involved in cell adhesion (14, 30). The fact that IgI-MBP, IgI *P. pastoris*, and IgII-MBP inhibited aggregation of mouse cerebellar neurons, whereas other Ig-like domains of NCAM had very little effect, further supports the notion that the IgI and IgII domains are involved in NCAM-mediated binding interactions. Our data are also in agreement with our recent prediction (5), based on the analysis of the three-dimensional structure of the IgI domain and the pre-

dicted three-dimensional structure of the IgII domain, that an acidic cluster of residues at the NH₂ terminus of the IgI domain (aspartic acid 29, 32, 34, 58, 59, and 84, and glutamic acid 85) and a basic cluster of residues of the IgII domain (lysine 135, 137, and 185, and arginine 139 and 171) may be involved in a symmetrical double-reciprocal binding (schematically depicted in Fig. 7a).

The estimated dissociation constant (K_D) of the interaction of the individual IgI and IgII domains was $5.5 \pm 1.6 \times 10^{-5}$ M. A rough estimate of the dissociation constant of the double-reciprocal interaction (K_D^{dr}) can be made. Let ΔG° be the standard Gibbs energy change of the interaction of the individual IgI and IgII domains at constant temperature and pressure. The standard Gibbs energy change of the double-reciprocal interaction, then, can be minimally estimated as $\approx 2\Delta G^\circ$, when the entropy loss associated with a more ordered complex is not taken into account, since the model (Fig. 7a) implies that the double-reciprocal interaction is symmetrical (5). The true value of the standard Gibbs energy change of the double-reciprocal interaction might be larger than $\approx 2\Delta G^\circ$ because of the entropy loss. Therefore

$$K_D^{dr} = \frac{e^{-\frac{2\Delta G^\circ}{RT}}}{e^{-\frac{\Delta G^\circ}{RT}} e^{-\frac{\Delta G^\circ}{RT}}} = K_D^2 \quad (\text{Eq. 6})$$

where R is the universal gas constant, and T is the absolute temperature. Thus, the dissociation constant of the double-reciprocal interaction for mouse NCAM can be minimally estimated as $3.3 \pm 1.8 \times 10^{-10}$ M based on the contributions of the individual domains, which is in reasonable agreement with the experimental value for rat NCAM 6.9×10^{-10} M (8).

The homophilic binding site for the chick transmembrane NCAM-B isoform has been mapped to a decapeptide sequence from Lys-243 to Glu-252 in the IgIII domain (9, 10), and the counterreceptor for the IgIII domain has been localized to the same decapeptide sequence (31). Recently, it has been demonstrated, in aggregation experiments with fluorescent microspheres, that the IgI, IgII, IgIII, IgIV, and IgV domains of chick NCAM interact with the IgV, IgIV, IgIII, IgII, and IgI domains, respectively (11). Our data indicate that there is possibly more than one mechanism of NCAM homophilic binding. However, in our experiments, no binding of the IgI, IgII, IgIII, IgIV, and IgV domains of mouse NCAM to the IgV, IgIV, IgIII, IgII, and IgI domains, respectively, using surface plasmon resonance analysis could be shown. The absence of binding may be the result of several factors: inactivation of the proteins during immobilization, purification, or storage; a very low affinity of the interaction; incorrect folding since the proteins were produced in bacteria and therefore not glycosylated. However, if five pairs of NCAM domains are involved in the homophilic binding at the same time (IgI binds to IgV, IgII to IgIV, IgIII to IgIII, IgIV to IgII, and IgV to IgI), and if the dissociation constants of the IgI-IgV, IgII-IgIV, and IgIII-IgIII interactions are approximately the same, then the K_D of the interaction of the individual domains is approximately the fifth root of the K_D of the homophilic binding of NCAM. Presuming that the K_D of the homophilic binding is as low as 10^{-10} M (100–1,000 times lower than the experimental value given in Ref. 8), then the K_D of the interaction of the individual domains is $\approx 10^{-2}$ M, which cannot be detected by surface plasmon resonance analysis. Although we cannot demonstrate that IgIII-MBP, IgIV-MBP, and IgV-MBP were folded correctly, we have several indications that that was the case for IgI-MBP and IgII-MBP. (i) Polyclonal antibodies of the first bleeding against IgI-MBP did not recognize a reduced NCAM preparation, whereas a nonreduced preparation was readily recognized, indicating that the conformation of the IgI domain in IgI-MBP was close to the conformation of the nonreduced form of NCAM, and therefore

that the disulfide bridge, which is an essential feature of an Ig-like domain, was formed. (ii) Both IgI-MBP and IgII-MBP inhibited aggregation of mouse cerebellar neurons, indicating that these protein constructs were functionally active. (iii) In contrast to the IgIII domain, the IgI and IgII domains are not glycosylated in native NCAM, and therefore, glycosylation is not required for proper folding. (iv) The binding of IgI-MBP and IgII-MBP to heparin, and of IgI-MBP to IgII-MBP, indicates that these protein constructs were folded in an active conformation.

Since the affinity of NCAM homophilic binding increases during development (8), probably because of a decrease in NCAM polysialylation (32, 33), it has been hypothesized that the homophilic binding mechanism is developmentally regulated by the PSA content of NCAM. Because PSA is attached to the IgV NCAM domain (34), the binding mechanism indicated by the model in Fig. 7a may be favored in a situation with a high PSA content, whereas NCAM molecules with a low amount of PSA may be able to slide along each other, favoring the mechanism in which all five Ig-like domains are involved: IgI binds to IgV, IgII to IgIV, IgIII to IgIII, IgIV to IgII, and IgV to IgI (11).

IgI *P. pastoris* was found to bind heparin with a constant of dissociation of $9.0 \pm 2.0 \times 10^{-7}$ M and association and dissociation rate constants of $1.1 \pm 0.3 \times 10^4$ M⁻¹ s⁻¹ and $8.4 \pm 0.4 \times 10^{-3}$ s⁻¹, respectively. No binding could be demonstrated to laminin, collagen type I, or fibronectin. Comparison of the heparin binding of IgI-MBP and IgII-MBP revealed that the IgII domain bound heparin with a higher affinity than the IgI domain. Heparin binding of the IgI domain may be considered specific on the following criteria. (i) The IgI domain bound heparin but did not bind other negatively charged carbohydrates such as carboxymethylated dextran (the surface of a CM5 sensor chip) and PSA. (ii) Other extracellular domains of NCAM (with the exception of the IgII domain) did not bind to heparin. In contrast to the IgII domain, where a cluster of basic amino acids capable of heparin binding has been identified, there is no cluster of basic amino acids in the IgI domain. It is possible that such a cluster may not be required for low affinity heparin-binding proteins.

It has been demonstrated previously that NCAM binds different types of collagen (12) and that binding of NCAM to collagens type I and V could be inhibited by glycosaminoglycans such as heparin and chondroitin sulfate (14). However, the authors were unable to determine whether the inhibition by glycosaminoglycans was the result of their binding to collagen or to NCAM. Therefore, it is not clear whether NCAM actually can bind collagen directly or via glycosaminoglycans. Neither IgI-MBP nor IgII-MBP bound to collagen type I directly. However, we demonstrated binding of IgI-MBP and IgII-MBP to collagen type I to which heparin was associated. In a competition experiment, heparin inhibited binding of IgI-MBP and IgII-MBP to the collagen-heparin complex, indicating that it was heparin and not collagen type I that bound IgI-MBP and IgII-MBP. Other NCAM domains did not bind to the collagen-heparin complex. The maximal binding of IgII-MBP to heparin alone was approximately 5 times higher than the maximal binding of IgI-MBP, whereas the maximal binding of IgII-MBP to the collagen-heparin complex was only 1.3 times higher than the maximal binding of IgI-MBP, indicating that IgI-MBP bound the collagen-heparin complex almost as well as IgII-MBP. This indicates that the IgI NCAM domain possibly also binds collagen type I although with a very low affinity.

Based on our data, we conclude that heparin can form a "bridge" between collagen type I and NCAM (Fig. 7b). In this model, both the IgI and IgII NCAM domains bind to heparin associated with collagen.

Thus, we present evidence that in mouse the Igl and IgII NCAM domains are directly involved in NCAM-mediated homophilic interaction. Both NCAM domains also bind heparin and, via heparin, collagen type I but probably not collagen type I directly.

REFERENCES

1. Krug, L., and Bock, E. 1992. *APMIS Suppl.* 27, 53-70.
2. Geglachy, G., and Bock, E. 1996. *Treatise on Biomembranes* 3, 33-75.
3. Cunningham, B. A., Hemperly, J. J., Murray, B. A., Prediger, E. A., Brackenbury, R., and Edelman, G. M. 1957. *Science* 236, 799-806.
4. Small, S. J., Shull, G. E., Santoni, M. J., and Akeson, R. 1987. *J. Cell Biol.* 105, 2335-2345.
5. Thomsen, N. K., Soroka, V., Jensen, P. H., Berezin, V., Kiselyov, V. V., Bock, E., and Poulsen, F. M. 1996. *Nature Struct. Biol.* 3, 581-584.
6. Rutishauser, U., Hoffman, S., and Edelman, G. M. 1982. *Proc. Natl. Acad. Sci. U.S.A.* 79, 685-689.
7. Hoffman, S., and Edelman, G. M. 1983. *Proc. Natl. Acad. Sci. U.S.A.* 80, 5762-5766.
8. Moran, N., and Bock, E. 1988. *FEBS Lett.* 242, 121-124.
9. Rao, Y., Wu, X.-F., Gariepy, J., Rutishauser, U., and Siu, C.-H. 1992. *J. Cell Biol.* 118, 937-949.
10. Rao, Y., Wu, X.-F., Yip, P., Gariepy, J., and Siu, C.-H. 1993. *J. Biol. Chem.* 268, 20630-20638.
11. Ranheim, T. S., Edelman, G. M., and Cunningham, B. A. 1996. *Proc. Natl. Acad. Sci. U.S.A.* 93, 4071-4075.
12. Probstmeier, R., Kuhn, K., and Schachner, M. 1989. *J. Neurochem.* 53, 1794-1801.
13. Cole, G. J., Schubert, D., and Glaser, L. 1985. *J. Cell Biol.* 100, 1192-1199.
14. Cole, G. J., and Glaser, L. 1986. *J. Cell Biol.* 102, 403-412.
15. Nybroe, O., Moran, N., and Bock, E. 1989. *J. Neurochem.* 52, 1947-1949.
16. Grumet, M., Flaccus, A., and Margolis, R. U. 1993. *J. Cell Biol.* 120, 815-824.
17. Cole, G. J., Loewy, A., Cross, N. V., Akeson, R., and Glaser, L. 1986. *J. Cell Biol.* 103, 1739-1744.
18. Cole, G. J., and Akeson, R. 1989. *Neuron* 2, 1157-1165.
19. Frei, T., von Bohlen und Halbach, F., Wille, W., and Schachner, M. 1992. *J. Cell Biol.* 118, 177-194.
20. Barthels, D., Santoni, M. J., Wille, W., Ruppert, C., Chaix, J. C., Hirsch, M. R., Fontecilla-Camps, J. C., and Goridis, C. 1987. *EMBO J.* 6, 907-914.
21. Santoni, M. J., Barthels, D., Barbas, J. A., Hirsch, M. R., Steinmetz, M., Goridis, C., and Wille, W. 1987. *Nucleic Acids Res.* 15, 8621-8641.
22. Kasper, C., Stahlhut, M., Berezin, V., Maar, T. E., Edvardsen, K., Kiselyov, V., Soroka, V., and Bock, E. 1996. *J. Neurosci. Res.* 46, 173-186.
23. Harboe, N., and Ingild, A. 1973. *Scand. J. Immunol. Suppl.* 2, 161-164.
24. Laemmli, U. K. 1970. *Nature* 227, 680-685.
25. Rasmussen, S., Ramlau, J., Axelsen, N. H., and Bock, E. 1992. *Scand. J. Immunol.* 15, 179-185.
26. Trenkner, E., and Sidman, R. L. 1977. *J. Cell Biol.* 75, 915-940.
27. Piez, K.-A. 1967. in *Treatise on Collagen* (Ramachandran, G. N., ed.) Vol. 1, pp. 207-252. Academic Press, London.
28. Buckholz, R. G., and Gleeson, M. A. G. 1991. *Bio. Technology* 9, 1067-1072.
29. Lindahl, U., and Hook, M. 1978. *Annu. Rev. Biochem.* 47, 385-417.
30. Frelinger, A. L., III, and Rutishauser, U. 1986. *J. Cell Biol.* 103, 1729-1737.
31. Rao, Y., Zhao, X., and Siu, C.-H. 1994. *J. Biol. Chem.* 269, 27540-27548.
32. Sadoul, R., Hirn, M., Deagostini-Bazin, H., Rougon, G., and Goridis, C. 1983. *Nature* 304, 347-349.
33. Rutishauser, U., Watanabe, M., Silver, J., Troy, F. A., and Vimr, E. R. 1985. *J. Cell Biol.* 101, 1842-1849.
34. Nelson, R. W., Bates, P. A., and Rutishauser, U. 1995. *J. Biol. Chem.* 270, 17171-17179.
35. Karlsson, R. 1994. *Anal. Biochem.* 221, 142-151.

**This Page is Inserted by IFW Indexing and Scanning
Operations and is not part of the Official Record.**

BEST AVAILABLE IMAGES

Defective images within this document are accurate representations of the original documents submitted by the applicant.

Defects in the images include but are not limited to the items checked:

- ☐ **BLACK BORDERS**
- ☐ **IMAGE CUT OFF AT TOP, BOTTOM OR SIDES**
- ☐ **FADED TEXT OR DRAWING**
- ☐ **BLURRED OR ILLEGIBLE TEXT OR DRAWING**
- ☐ **SKEWED/SLANTED IMAGES**
- ☐ **COLOR OR BLACK AND WHITE PHOTOGRAPHS**
- ☐ **GRAY SCALE DOCUMENTS**
- ☐ **LINES OR MARKS ON ORIGINAL DOCUMENT**
- ☒ **REFERENCE(S) OR EXHIBIT(S) SUBMITTED ARE POOR QUALITY**
- ☐ **OTHER:** _____

IMAGES ARE BEST AVAILABLE COPY.

As rescanning these documents will not correct the image problems checked, please do not report these problems to the IFW Image Problem Mailbox.

This Page Blank (uspto)